DOI: https://doi.org/10.57233/ijsgs.v12i1.1076 ISSNp: 2488-9229; ISSNe: 3027-1118

IJSGS FUGUSAU VOL. 12(1) WEBSITE: https://fugus-ijsgs.com.ng

INTERNATIONAL JOURNAL OF SCIENCE FOR GLOBAL SUSTAINABILITY

(A PUBLICATION OF FACULTY OF SCIENCE, FEDERAL UNIVERSITY GUSAU, NIGERIA)

MHD Casson Fluid Flow over an Infinite Vertical Plate with Suction/Injection and Viscous Dissipation.

[1]Maduka, N. C. and [2]Omokhuale, Emmanuel

[1]Department of Physics, Federal University Gusau, P. M. B. 1001, Zamfara State, Nigeria.

[2]Department of Mathematical Sciences, Federal University Gusau, P. M. B. 1001, Zamfara State, Nigeria.

Corresponding Author's Email: emmanuelomokhuale@fugusau.edu.ng , emmanuelomokhuale@gmail.com

Received on: March, 2026 **Revised and Accepted on:** March, 2026 **Published on:** March, 2026

ABSTRACT

This study examines the magnetohydrodynamic (MHD) flow of a Casson fluid over an infinite vertical plate incorporating the combined effect of suction/injection, chemical reaction and viscous dissipation, thermal radiation. The governing nonlinear partial differential equations (PDEs) in dimensional form are transformed to non-dimensional form and finite difference method (EFDM) is used to numerically obtain approximations for the velocity, temperature and concentration of the fluid. Computations were performed to study the effect of key parameters embedded in the flow quantities. The results are shown graphically and discussed. It is observed that fluid velocity increases when thermal radiation, viscous dissipation, heat generation, Casson parameters, and Grashof numbers (thermal and mass) become stronger. Conversely, fluid velocity slows down as Prandtl numbers and magnetic parameters increase. Comparison of present results with the previous literature was carried out to show the accuracy of the results.

Keywords: Casson fluid; EFDM; MHD; suction and injection.

1.0 INTRODUCTION

Magnetohydrodynamics is the study of the behavior of the electrically conducting fluids. It is based on this concept that magnetic fluids are able to induce currents in a moving conductive fluid. The issues on magnetohydrodynamics thick liquids have significant in designing applications like MHD generators and MHD gas pedals, research center plasmas, the pivoting stream of liquids with the occurrence of attractive field is happened in cosmical and geophysical liquid elements, the sun-oriented material science engaged with the sunspot advancement, sun-based cycle and construction of turning the attractive stars (Prameela *et al.*, 2022). Jabeen and Liaquat (2026) examined the magnetohydrodynamic (MHD) flow of a Casson nanofluid over a permeable stretching sheet incorporating the combined influence of suction/injection, ohmic and viscous dissipation, thermal radiation, and Arrhenius activation energy. Alotaibi *et al.* (2020) introduced the effect of heat absorption (generation) and suction (injection) on magnetohydrodynamic (MHD) boundary-layer flow of Casson nanofluid (CNF) via a non-linear stretching surface with the viscous dissipation in two dimensions. They utilized similarity transformations, their leading PDEs were transformed into a set of ODEs with adequate boundary conditions and then resolved numerically.

Due to its large number of applications, the study of non-Newtonian fluids over an extending surface has attained great attention. In fact, the impacts of non-Newtonian behavior can be assessed by its elasticity, but their constitutive equations sometimes identify the rheological properties of the fluid. Provided the rheological parameters, the constitutive equations in the non-Newtonian fluids are more complex and thus giving rise to the complicated equations than the Navier–Stokes equations. Many of the liquids utilized in the oil sector, multiplex networks, cooling processes of micro-ships, open-flow switching, and simulating reservoirs are considerable non-Newtonian. Casson fluid has special characteristics in the class of non-Newtonian fluids, which are commonly used in food manufacturing, metallurgy, drilling, and bio-engineering activities, etc. (Alotaibi *et al.*, 2020). The flow characteristics of non-Newtonian fluids, such as the Casson fluid, are considerably different from those of Newtonian fluids. Whereas the viscosity of Newtonian fluids is constant independent of shear rate, the viscosity of non-Newtonian fluids depends on the applied stress or shear conditions. This characteristic has made non-Newtonian fluids suitable for specific applications in which fluid dynamics and heat transfer operations need to be controlled. Many studies on Casson fluid appeared because of its ability to model biological fluids such as blood and its usefulness in various industrial processes that include complex rheological properties (Rafiq *et al.*, 2025). Omokhuale and Altine (2017) studied Casson fluid flow and mass transfer along a porous medium using perturbation method. Abo-Dahab *et al.* (2021) executed to explicate thermophysical aspects of viscoelastic fluid flow produced by a nonlinearized stretched surface. In their work, viscoelasticity is characterized by Casson fluid model and expressed rheologically in momentum equation. Flow attributes of Casson fluid are thoroughly investigated under transversal magnetized field and along with provision of suction/injection to surface. Venkata Ramudu *et al.* (2020) analyzed heat transfer characteristics of a steady two-dimensional magnetohydrodynamic shear thickening Casson fluid across a vertical stretching sheet in the presence of variable heat source/sink. They also considered the impact of thermal radiation and velocity slip.

Suction and blowing are crucial mechanisms for controlling and optimizing non-Newtonian fluid flow over a porous flat plate. They significantly enhance heat and mass transfer, regulate boundary layer development, reduce drag, and improve flow stability. Suction reduces the boundary layer

DOI: https://doi.org/10.57233/ijsgs.v12i1.1076 ISSNp: 2488-9229; ISSNe: 3027-1118

thickness, minimizing flow separation and increasing stability. This can delay or prevent turbulence, enhancing overall system performance. Suction also improves heat transfer by thinning the thermal boundary layer, enabling more efficient cooling or heating. This is especially beneficial in processes involving temperature-dependent non-Newtonian fluids, such as nanofluids or fluids with complex rheological behaviors like those described by the Carreau or Cross models. Reducing the boundary layer thickness through suction also lowers skin friction drag, improving energy efficiency in applications like fluid transport or external flow over surfaces. Moreover, suction stabilizes the boundary layer by reducing velocity fluctuations, which delays the transition to turbulence. This stabilization is critical in non-Newtonian fluid flows, where turbulence can significantly impact flow behavior and system performance. Blowing, on the other hand, introduces additional fluid into the boundary layer, increasing its thickness. Depending on the strength of the blowing, this can either stabilize or destabilize the flow. Blowing can also regulate surface temperature by introducing cooler or warmer fluid into the boundary layer, which is valuable in processes requiring precise thermal management, such as industrial cooling or biotechnological applications. Although blowing may increase drag, controlled blowing can help achieve a desired shear stress distribution, potentially reducing flow resistance in specific regions. Additionally, the strength of blowing determines its impact on the transition to turbulence, which it can either delay or accelerate (Jayaprakash *et al.*, 2025).

Rehman *et al.* (2019) gave a mathematical model of the non-Newtonian Casson liquid over an unsteady stretching sheet under the combined effects of different natural parameters with heat transfer in the presence of suction/injection phenomena. The movement of a laminar thin liquid film and associated heat transfer from a horizontal stretching surface is studied. Magnetic field is proposed perpendicular to the direction of flow, while surface tension is varied quadratically with temperature of the conducting fluid. Further, variable viscosity and thermal conductivity (linear function of temperature) of the flow are examined. Sampath Kumar and Pai (2019) studied the effect of injection and suction on velocity profile, skin friction and pressure distribution of a Casson fluid flow between two parallel infinite rectangular plates approaching or receding from each other with suction or injection at the porous plates. The governing Navier–Stokes equations in their work are reduced to the fourth-order non-linear ordinary differential equation through the similarity transformations. The approximated analytic solution based on the Homotopy perturbation method is given and also compared with the classical finite difference method. Paul, A., & Nath (2024) investigated stagnation point flow characteristics of magneto-hydrodynamic (MHD) Cason-Williamson hybrid nanofluids over an exponentially stretched cylinder, incorporating phenomena like viscous dissipation and suction/injection effects, as no prior investigation has been conducted on it, which represents the distinctiveness of the flow model.

Finite difference methods is very useful in solving coupled non-linear partial differential equations whose solutions cannot be obtained analytically. Explicit Finite difference method (EFDM) is very useful in solving coupled non-linear partial differential equations whose solutions cannot be obtained analytically. Mondal *et al.* (2019) conducted a numerical exploration on inscribed MHD unsteady heat and mass transfer of Casson nanofluid flow where variable thermal conductivity, radiation and heat absorption are counterfeited using EFDM. Omokhuale and Jabaka (2019) studied magnetohydrodynamic Casson fluid flow over an infinite vertical plate with chemical reaction and heat generation numerically using EFDM. They extended their studies and considered radiation, variable thermal conductivity and chemical absorption in (Omokhuale and Jabaka, 2020a; Omokhuale and Jabaka, 2020b).

In all the above studies mentioned, the situations are which the solutions of Casson fluid were mostly obtained analytically. There are few instances in which the numerical schemes were employed. The present work aims to fill the gap in the existing literatures. Therefore, motivated by the above studies and applications mentioned. Omokhuale and Jabaka (2020a) is extended; we shall study magnetohydrodynamic Casson fluid flow past a vertical plate in the presence of heat dissipation, suction/injection numerically using EFDM.

2.0 MATHEMATICAL FORMULATION

We consider Casson fluid over an infinite vertical plate embedded in a saturated porous medium. The flow being restricted to $y > 0$, where y is the coordinate which would be measured in the normal direction to the plate. The fluid would be assumed to be electrically conducting with a uniform magnetic field B of strength B_0, applied in a direction perpendicular to the plate. The plate temperature is raised to T_w which is thereafter maintained constant.

The rheological equation of state for the Cauchy stress tensor of Casson fluid will be given by,

$$\tau = \tau_0 + \mu\tau^*$$

where $\tau_0 = \begin{cases} 2\left(\mu_B + \dfrac{p_y}{\sqrt{2\pi}}\right)e_{ij}, \ when \ \pi > \pi_c \\ 2\left(\mu_B + \dfrac{p_y}{\sqrt{2\pi_c}}\right)e_{ij}, \ when \ \pi < \pi_c \end{cases}$

DOI: https://doi.org/10.57233/ijsgs.v12i1.1076 ISSNp: 2488-9229; ISSNe: 3027-1118

IJSGS FUGUSAU VOL. 12(1) WEBSITE: https://fugus-ijsgs.com.ng

where $\pi = e_{ij}e_{ij}$ and e_{ij} is the $(i, j)^{th}$ component of the deformation rate.

The following assumptions were made before deriving the governing equations; incompressible flow, free convection and non-Newtonian flow, infinite vertical plate, fluid suction/injection and magnetic field are imposed at the plate surface, the temperature and concentration of the fluid are raised to T'_w and C'_w respectively and are higher than the ambient temperature and that of fluid. In addition, the effects of chemical reaction, radiation are considered. It is also assumed that the viscous dissipation is present.

The governing equations of the flow under the usual Boussinesq and boundary-layer approximation can be written as:

$$\frac{\partial v'}{\partial y'} = 0 \tag{1}$$

$$\rho\left(\frac{\partial u'}{\partial t'} + v'\frac{\partial u'}{\partial y'}\right) = \mu_B\left(1+\frac{1}{\gamma}\right)\frac{\partial^2 u'}{\partial y'^2} - \sigma B_0^2 u' - \frac{\mu\eta}{K_1}\left(1+\frac{1}{\gamma}\right)u' + g\rho\left[\beta_T\left(T'-T'_\infty\right)+\beta_m\left(C'-C'_\infty\right)\right] \tag{2}$$

$$\left(\frac{\partial T'}{\partial t'} + v'\frac{\partial T'}{\partial y'}\right) = \frac{k}{\rho Cp}\frac{\partial^2 T'}{\partial y'^2} - \frac{1}{\rho Cp}\frac{\partial q_r}{\partial y^*} + \frac{Q}{\rho Cp}\left(T'-T'_\infty\right) + \frac{\mu}{Cp}\left(\frac{\partial u'}{\partial y'}\right)^2 \tag{3}$$

$$\frac{\partial C'}{\partial t'} + v'\frac{\partial C'}{\partial y'} = D\frac{\partial^2 C'}{\partial y'^2} - R^*\left(C'-C'_\infty\right) \tag{4}$$

with the following initial and boundary conditions:

$$\left.\begin{aligned} &t' \le 0, u' = 0, T' \to T'_\infty, C' \to C'_\infty \ \text{for all } y' \\ &t' > 0, u' = u_p, T' = T'_w, C' = C'_w \ \text{at } y' = 0 \\ &u' \to 0, T' \to T'_\infty, C' \to C'_\infty \ \text{as } y' \to \infty \end{aligned}\right\} \tag{5}$$

$v_0 > 0$ is the suction parameter and $v_0 < 0$ is the injection parameter.

For the case of an optically thin gray gas the local radiant absorption is expressed by

$$\frac{\partial q_r}{\partial y'} = -4a_R\sigma\left(T'^4_\infty - T'^4\right) \tag{6}$$

we assume that the temperature difference within the flow are sufficiently small such that T'^4 may be expressed as a linear function of the temperature. This is accomplished by expanding T'^4 in Taylor series about T'_∞ and neglecting higher-order terms, thus

$$T'^4 \cong 4T'^3_\infty T' - 3T'^4_\infty \tag{7}$$

By using equations (6) and (7), equation (2) reduces to

$$\left[\frac{\partial T'}{\partial t'} + v\frac{\partial T'}{\partial y'}\right] = \frac{k_0}{\rho Cp}\frac{\partial^2 T'}{\partial y'^2} - \frac{16a_R\sigma T'^3_\infty}{\rho Cp}\left(T'-T'_\infty\right) + \frac{Q}{\rho Cp}\left(T'-T'_\infty\right) + \nu\left(\frac{\partial u'}{\partial y'}\right)^2 \tag{8}$$

On introducing the following non-dimensionless quantities

$$\left.\begin{aligned} Y = \frac{u_0}{\nu}y', u_p = \frac{u'_p}{u_0}, t = \frac{u_0^2}{\nu}t', U = \frac{u'}{u_0}, \chi = \frac{T'-T'_\infty}{T_w-T_\infty}, \eta = \frac{C'-C'_\infty}{C_w-C_\infty}, \tau^* = \frac{\tau}{\rho u^2} \end{aligned}\right\} \tag{9}$$

Using (1) and (9), equations (3) - (5) and (8) is transformed to:

$$\frac{\partial U}{\partial t} \pm \lambda\frac{\partial U}{\partial Y} = \left(1+\frac{1}{\gamma}\right)\frac{\partial^2 U}{\partial Y^2} + G_1\chi + G_2\eta - \left[M^2 + \left(1+\frac{1}{\gamma}\right)\frac{1}{K}\right]U \tag{10}$$

$$\frac{\partial \chi}{\partial t} \pm \lambda\frac{\partial \chi}{\partial Y} = \frac{1}{\Pr}\frac{\partial^2 \chi}{\partial Y^2} - \frac{R}{\Pr}\chi + \xi\chi + Ec\left(\frac{\partial U}{\partial Y}\right)^2 \tag{11}$$

DOI: https://doi.org/10.57233/ijsgs.v12i1.1076 ISSNp: 2488-9229; ISSNe: 3027-1118

IJSGS FUGUSAU VOL. 12(1) WEBSITE: https://fugus-ijsgs.com.ng

$$\frac{\partial \eta}{\partial t} \pm \lambda \frac{\partial \eta}{\partial Y} = \frac{1}{Sc}\frac{\partial^2 \eta}{\partial Y^2} - \gamma \eta \tag{12}$$

The corresponding boundary conditions are:

$$\left.\begin{aligned} &U = 0, \chi = 0, \eta = 0 \ for\ all\ Y, t \le 0 \\ &U = u_p, \chi = 1, \eta = 1 \ at\ Y = 0 \\ &U \to 0, \chi \to 0, \eta \to 0\ as\ \mathrm{Y} \to \infty \end{aligned}\right\} \tag{13}$$

where γ is the Casson parameter, G_1 is the thermal Grashof number, G_2 is the mass Grashof number, Sc is the Schmidt number, Pr is the Prandtl number, M is the magnetic parameter, γ is the chemical reaction parameter, K is the permeability parameter, λ is the suction parameter, ξ is the heat generation parameter, Ec is the Eckert number.

3.0 COMPUTATIONAL TECHNIQUE

To get the difference equations, the region of the flow is divided into a grid or mesh of line parallel to Y axis. Where Y-axis is normal to the plate. It is considered that the plate is of height $Y_{\max} = 150$ i.e. Y varies from 1 to 150. There are $m = 150$ and $n = 300$ grid spacing in the Y-directions. It is assumed that Δy is a constant mesh size along Y direction and taken as $\Delta Y = 0.50\left(0 \le Y \le 150\right)$. with the smaller time-step, $\Delta t = 0.0005$ and u', T' and C' represents the values of U, χ and η at the end of a time step, respectively.

Therefore, the nonlinear coupled partial differential equations (10) to (12) subject to boundary conditions (13) are solved numerically using explicit finite difference method as below:

$$\left(\frac{U'_{i,j} - U_{i,j}}{\Delta t} \pm \lambda \frac{U_{i,j+1} - U_{i,j}}{\Delta Y}\right) = \left(1 + \frac{1}{\gamma}\right)\left[\frac{U_{i,j+1} - 2U_{i,j} + U_{i,j-1}}{\left(\Delta Y\right)^2}\right] - M\left(U_{i,j}\right) - \frac{1}{K}\left(U_{i,j}\right) + G_1\left(\chi_{i,j}\right) + G_2\left(\eta_{i,j}\right) \tag{14}$$

$$\left(\frac{\chi'_{i,j+1} - \chi_{i,j}}{\Delta t} \pm \lambda \frac{\chi_{i,j+1} - \chi_{i,j}}{\Delta Y}\right) = \frac{1}{\mathrm{Pr}} \cdot \left[\frac{\chi_{i,j+1} - 2\chi_{i,j} + \chi_{i,j-1}}{\left(\Delta Y\right)^2}\right] - \frac{R}{\mathrm{Pr}}\left(\chi_{i,j+1} + \chi_{i,j}\right) + \xi\left(\chi_{i,j+1} + \chi_{i,j}\right) + Ec\left(\frac{U_{i,j+1} - U_{i,j}}{\Delta Y}\right)^2 \tag{15}$$

$$Sc\left(\frac{\eta'_{i,j} - \eta_{i,j}}{\Delta t} \pm \lambda \frac{\eta_{i,j+1} - \eta_{i,j}}{\Delta Y}\right) = \left[\frac{\eta_{i,j+1} - 2\eta_{i,j} + \eta_{i,j-1}}{\left(\Delta Y\right)^2}\right] - \frac{\gamma Sc}{2}\left(\eta_{i,j}\right) \tag{16}$$

The initial and boundary conditions becomes

$$\left.\begin{aligned} &U_{i,0} = 0, \chi_{i,0} = 0, \eta_{i,0} = 0 \ \text{for all i except } i = 0 \\ &U_{i,0} = u_p, \chi_{i,0} = 1, \eta_{i,0} = 1 \\ &U_{L,0} = 0, \chi_{L,0} = 1, \eta_{L,0} = 1 \end{aligned}\right\} \tag{17}$$

where L corresponds to ∞. The suffix i corresponds to η and j is equals to t. consequently, $\Delta t = t_{j+1} - t_j$ and $\Delta Y = Y_{i+1} - Y_i$.

The finite difference approximations of these equations were solved by using the values for G_1 = G_2 = M = $\delta = \lambda$ = 1, $\gamma = 0.5$, $\xi = 0.5$, Pr = 0.71, Sc = 0.6, Ec = 0.2, χ = 0.5, K= 0.5, except where they are varied. A step size of ΔY = 0.01 is used for the interval $Y_{\min}$ = 0 to $Y_{\max}$ = 6 for a desired accuracy and a convergence criterion of 10^{-6} is satisfied for various parameters.

DOI: https://doi.org/10.57233/ijsgs.v12i1.1076 ISSNp: 2488-9229; ISSNe: 3027-1118

IJSGS FUGUSAU VOL. 12(1) WEBSITE: https://fugus-ijsgs.com.ng

4.0 RESULTS AND DISCUSSION

An explicit finite difference technique has been adopted to obtain the numerical results of the present model has been carried out for the different values of parameters embedded on the velocity, temperature and concentration within the boundary conditions. The finite difference approximations of these equations were solved by using the values for G_1 = G_2 = M = $\delta = \lambda = 1, \gamma = 0.5$, $\xi = 0.5$, Pr = 0.71, Sc = 0.6, Ec = 0.2, χ = 0.5, K= 0.5, except where they are varied. The interval Y_{min} = 0 to Y_{max} = 6 for a desired accuracy and a convergence for various parameters.

Figures 1 to 10 show the velocity profiles with different parameters, respectively.

Figure 1 depicts the effect of Prandtl number on the velocity. It is observed that, the velocity falls with increasing Prandtl number. Effect of Magnetic parameter M on the velocity is displayed in Figure 2, it is seen that, the velocity reduces with significance of magnetic effect. This occurs because of the application of transverse magnetic field to an electrically conducting fluid which cause a Lorentz force (a resistive type force) same with drag force which leads to the deceleration of the flow. Casson parameter effect on the velocity profile is presented in Figure 3. It is found that, the velocity rises with increasing Casson parameter. It is interesting to note that Casson parameter makes the velocity boundary layer thickness thicker. This occurs because of the plasticity of Casson fluid. Effects of suction and injection parameters on the velocity are presented in Figures 4 and 5, respectively. It is clear that, the velocity is lower due to an increase in suction parameter and an opposite trend occurs when injection is raised, respectively. Figures 6 and 7 illustrate the effects of different values of thermal and mass Grashof numbers on the velocity, respectively, it is obvious that, the velocity rises with increasing thermal and mass Grashof number, respectively. Buoyancy force acts like a favourable pressure gradient which accelerates the fluid within the boundary layer.

In Figure 8, the effect of heat dissipation on the velocity is provided. It is found that, the velocity becomes higher with rise in viscous dissipation. The variation of heat generation parameter on the momentum boundary layer is shown in Figure 9. It is seen that, the velocity is significant due to rise in heat generation within the boundary. with respect to temperature profile is shown in Figure 10. The increment in chemical absorption parameter increases the velocity of the fluid. This is due to the fact that chemical absorption of surface increases which leads velocity profile to grow up. The effect of thermal radiation on the momentum boundary of the fluid is illustrated in Figure 11. It is observed that, increase in the thermal radiation lead to rise in the fluid's velocity.

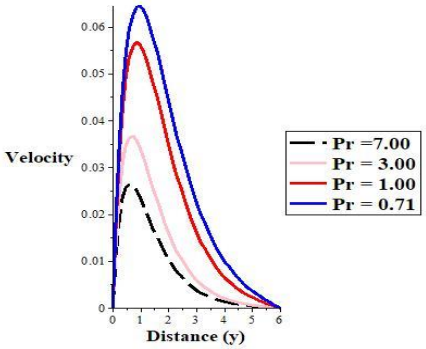

Figure 1: Effect of Prandtl number on velocity

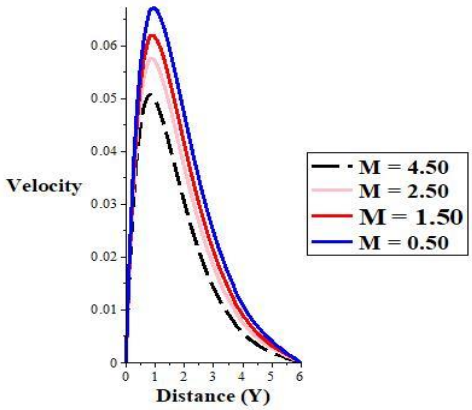

Figure 2: Effect of Magnetic parameter on velocity

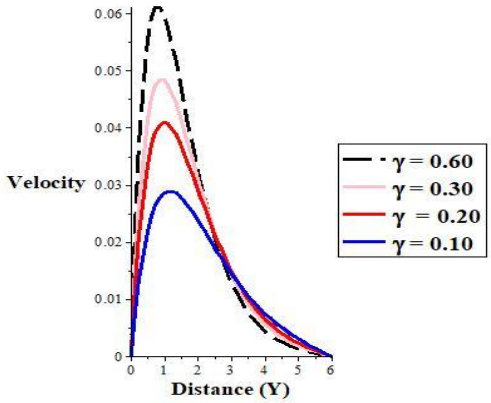

Figure 3: Effect of Casson parameter on velocity

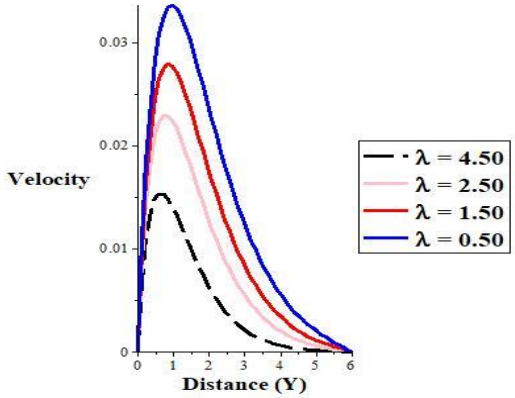

Figure 4: Effect of Suction parameter on velocity

DOI: https://doi.org/10.57233/ijsgs.v12i1.1076 ISSNp: 2488-9229; ISSNe: 3027-1118

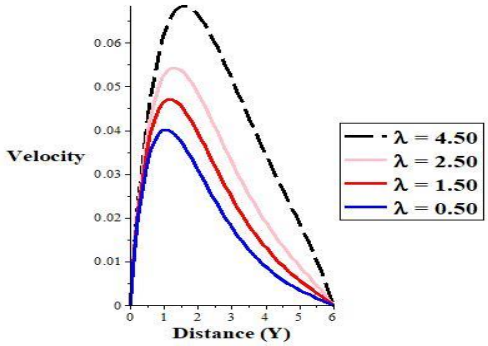

Figure 5: Effect of Injection parameter on velocity

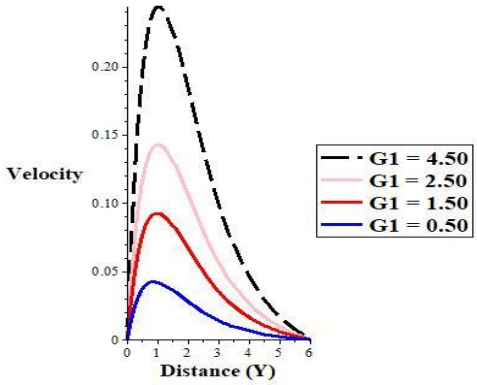

Figure 6: Effect of thermal Grashof number on velocity

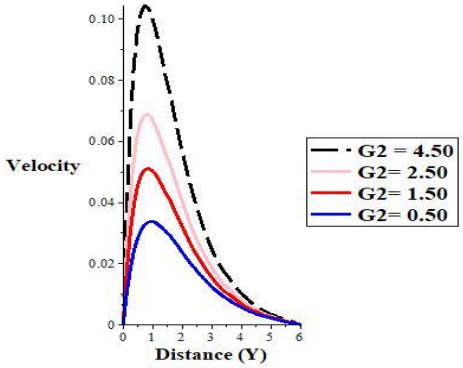

Figure 7: Effect of mass Grashof number on velocity

Figures 11 and 12 gives the temperature profiles. In Figure 11, the effect of heat generation on the temperature is shown. It is observed that, the temperature increases when the heat generation rises. Figure 12 connotes the effect of

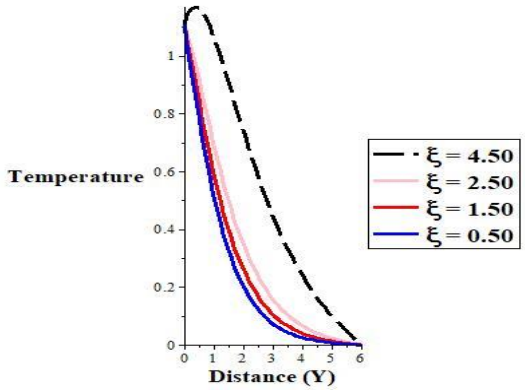

Figure 11. Effect of heat generation on Temperature

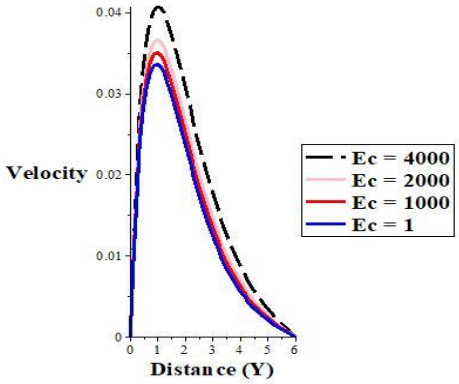

Figure 8: Effect of heat dissipation on velocity

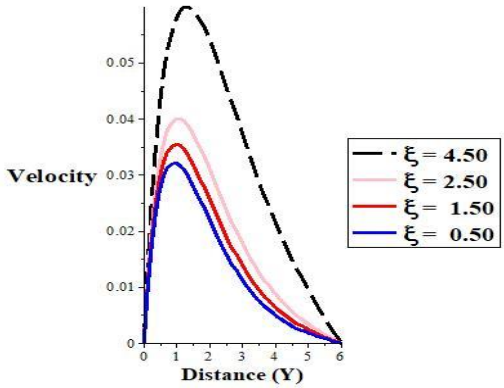

Figure 9: Effect of heat generation on velocity

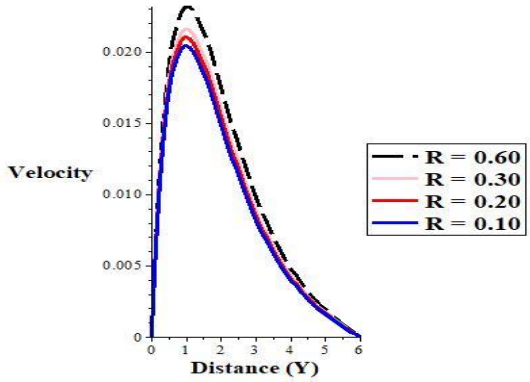

Figure 10: Effect of heat radiation on velocity

viscous dissipation on the temperature of the fluid. It is clear that, the temperature is higher as heat dissipates within the boundary layer.

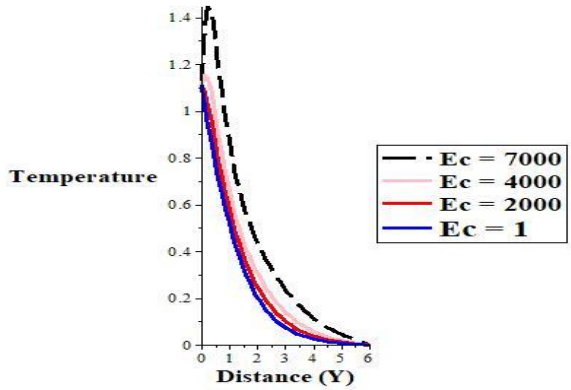

Figure 12: Effect of heat dissipation on Temperature

DOI: https://doi.org/10.57233/ijsgs.v12i1.1076 ISSNp: 2488-9229; ISSNe: 3027-1118

IJSGS FUGUSAU VOL. 12(1) WEBSITE: https://fugus-ijsgs.com.ng

Effect of chemical reaction with respect to concentration is visualized in Figure 13. As Schmidt number is the ratio of viscous diffusion rate to mass diffusion rate. It is demonstrated that, the concentration is lower as the chemical reaction parameter is increased.

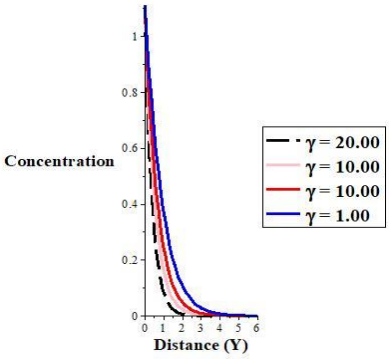

Figure 13. Effect of chemical reaction on Concentration.

5.0 CONCLUSION

Magnetohydrodynamic (MHD) flow of a Casson fluid over an infinite vertical plate incorporating the combined effect of suction/injection, chemical reaction and viscous dissipation, thermal radiation was examined. The flow was governed by a modeled coupled nonlinear system of partial differential equations (PDEs) in dimensional form which are transformed into dimensionless form using suitable variables. EFDM was used to obtain approximates for the fluid's velocity, temperature, concentration. Key findings are as follows:

1. Velocity of the fluid rises when thermal radiation, Casson, viscous dissipation, heat generation parameters and thermal and mass Grashof numbers become significant while an opposite trend happen with increasing values of Prandtl number and magnetic parameter.
2. Concentration boundary layer thickness reduces due to higher chemical reaction.
3. The temperature of the fluid become higher as both heat dissipation and generation are raised, respectively.

6.0 ACKNOWLEDGEMENTS

The authors are grateful to Tertiary Education Trust Fund (TETFUND) and the management of Federal University Gusau, Nigeria. for funding this research work under the Institutional Based Research **(TETF/DR&D/CE/UNI/GUSAU/IBR/2026/VOL.1)**.

REFERENCES

Abo-Dahab, S. M., Abdelhafez, M. A., Mebarek-Oudina, F., & Bilal, S. M. (2021). MHD Casson nanofluid flow over nonlinearly heated porous medium in presence of extending surface effect with suction/injection: SM Dahab et al. *Indian Journal of Physics*, *95*(12), 2703-2717. https://doi.org/10.1007/s12648-020-01923-z

Alotaibi, H., Althubiti, S., Eid, M. R., & Mahny, K. L. (2020). Numerical treatment of MHD flow of Casson nanofluid via convectively heated non-linear extending surface with viscous dissipation and suction/injection effects. *Comput. Mater. Continua*, *66*(1), 229-245. https://doi.org/10.1186/s13661-019-1133-0

Jabeen, K., & Liaquat, A. (2026). Suction/Injection Analysis of MHD Bioconvective Casson Fluid Flow Over a Darcy–Forchheimer Porous Stretching Sheet With Thermal Radiation, Double Diffusion, and Ohmic–Viscous Dissipation Effects. *Heat Transfer*. https://doi.org/10.1002/htj.70278

Jayaprakash, J., Govindan, V., & Byeon, H. (2025). Effect of activation energy on Casson–Maxwell fluid via porous media including blowing and suction mechanisms. *Partial Differential Equations in Applied Mathematics*, *13*, https://doi.org/10.1016/j.padiff.2024.101060

Omokhuale, E. and Altine, M. M. (2017). Casson fluid flow and mass transfer along a porous medium using perturbation method. *The Journal of the Mathematical Association of Nigeria (Abacus), Mathematics Science Series*, 44(1), 334 – 343.

Omokhuale, E., & Jabaka, M. L. (2019). Magnetohydrodynamic Casson Fluid Flow over an Infinite Vertical Plate with Chemical Reaction and Heat Generation. *American Journal of Computational Mathematics*, *9*(3), 187-200. https://doi.org/10.4236/ajcm.2019.93014

Omokhuale, E., & Jabaka, M. L. (2020a). Magnetohydrodynamic Casson Fluid Flow Past a Vertical Plate in the Presence of Thermal Conductivity and Chemical Absorption. *International Journal of Science for Global Sustainability*, *6*(2), 82-91. https://doi.org/10.57233/ijsgs.v6i2.111

Omokhuale, E., & Jabaka, M. L. (2020b). Effect of Radiation on Heat and Mass Transfer Magnetohydrodynamic Casson fluid flow in a vertical channel. *CaJoST*, *2*(2), 73-80.

Paul, A., & Nath, J. M. (2024). Magneto-hydrodynamic stagnation point flow of casson williamson hybrid nanofluid incorporating viscous dissipation and suction/injection effect past an exponentially stretching cylinder. *Journal of Nanofluids*, *13*(3), 710-720. https://doi.org/10.1166/jon.2024.2162

Prameela, M., Gangadhar, K., & Reddy, G. J. (2022). MHD free convective non-Newtonian Casson fluid flow over an oscillating vertical plate. *Partial Differential Equations in Applied Mathematics*, *5*. https://doi.org/10.1016/j.padiff.2022.100366

Rafiq, S., Bilal, B. A., Afzal, A., Tawade, J. V., Kulkarni, N. V., Abdullaeva, B., ... & Gupta, M. (2025). Thermo-fluid dynamics of non-Newtonian Casson fluid in expanding-contracting channels with joule heating and variable thermal properties. *Partial Differential Equations in Applied Mathematics*, *13*. https://doi.org/10.1016/j.padiff.2025.101105

Rehman, S., Idrees, M., Shah, R. A., & Khan, Z. (2019). Suction/injection effects on an unsteady MHD Casson thin film flow with slip and uniform thickness over a stretching sheet along variable flow properties. *Boundary Value Problems*, *2019*(1), 26. https://doi.org/10.1186/s13661-019-1133-0

Sampath Kumar, VS & Pai, N. P. (2019). Suction and injection effect on flow between two plates with reference to Casson fluid model. *Multidiscipline Modeling in Materials and Structures*, *15*(3), 559-574. https://doi.org/10.1108/MMMS-05-2018-0092

Venkata Ramudu, A. C., Anantha Kumar, K., Sugunamma, V., & Sandeep, N. (2020). Influence of suction/injection on MHD Casson fluid flow over a vertical stretching surface. *Journal of Thermal Analysis and Calorimetry*, *139*(6), 3675-3682. https://doi.org/10.1007/s10973-019-08776-7